The search for the dark vector boson via the Higgs portal

P Ntsoele

University of Johannesburg, Johannesburg, Mechanical Engineering, South Africa

E-mail: `pntsoele@uj.ac.za`

Abstract. The Standard Model (SM) is known to be incomplete (it cannot explain dark matter, dark energy, gravitational waves, matter-antimatter asymmetry, etc). The introduction of a Dark Sector via an additional $U(1)_d$ gauge symmetry added to the SM Lagrangian could be the long-awaited solution. In this model there is a dark vector boson Z_d which can mix with the SM hypercharge gauge boson. This opens the Hypercharge Portal which can mediate the fluctuation of a Z to a Z_d, or the decay of the Z_d to SM leptons. If a dark Higgs singlet also exists, then this breaks the $U(1)_d$ symmetry, allowing for Higgs mixing (parametrised by κ) between the SM and dark sector Higgs bosons, and thereby opening the Higgs portal as a discovery channel. Including dark fermionic fields in the Lagrangian allows for long-lived cold Dark Matter candidates. The various connections between the Dark and SM sectors allow descriptions of many key astro-physical phenomena. The Model is therefore a fascinating candidate for new physics beyond the SM. It becomes crucial to search for experimental signatures of this model. This contribution discusses an ATLAS search for the dark force boson Z_d using its production via the Higgs Portal and its decay back to SM leptons: $H \to Z_d Z_d \to 4\ell$.

1. Introduction

The search for the Z_d dark force particle is inspired by a class of models where the Standard Model (SM) is extended by introducing hidden or dark sector states [1, 2, 3, 4, 5, 6, 7, 8, 9, 10], in a way that provides candidates for dark matter [11] and dark forces which accommodate both the indirect and the (potential) direct evidence based on astronomical observations or space platform experiments [12, 13, 14]. The hidden or dark sector is introduced in this case with an additional $U(1)_d$ dark gauge symmetry [5, 6, 7, 8, 9, 10].

If the primary route for the production of dark particles in the search, proceeds from the prior production of the Higgs particle, then we have also specialised to the Higgs Portal class of models. In this case we assume the dark sector coupling to the SM through kinetic mixing with the hypercharge boson via the kinetic mixing parameter ϵ to be very small. This is because ϵ allows for processes like $Z \longrightarrow Z_d$ and $Z_d \to \ell\ell$, which must already be constrained by the current excellent agreement between the SM and electroweak precision observables, $\epsilon \lesssim 10^{-4}$ [5, 6, 7, 8, 9, 10, 15, 16]. We introduce a Higgs level coupling between the dark sector and the SM. The $U(1)_d$ symmetry of the dark sector is broken by the introduction of a dark Higgs boson, which can mix with the SM Higgs boson [5, 6, 7, 8, 9, 10] with a coupling strength κ. The observed Higgs boson would then be the lighter partner of the new Higgs doublet, which can also decay via the dark sector. We then conceptually allow the decay $H \to h_d \to Z_d Z_d$. We also assume the dark fermions are sufficiently heavy $m_{f_d} < m_{Z_d}/2$, so that the branching ratio for the decay $Z_d \to \ell\ell$ may be taken as 100%, even though the kinetic mixing parameter ϵ has been set small. The Higgs Portal has been opened by the observation of the discovered Higgs at 125 GeV [17, 18, 19] during Run 1 of the Large Hadron Collider (LHC) [20, 21]. This has ushered in a new and rich experimental program for physics beyond the SM.

This paper describes the recently published Run 2 search for the Higgs boson decaying to four

leptons via two Z_d bosons using pp collision data at $\sqrt{s} = 13$ TeV corresponding to an integrated luminosity of 36.1 ± 1.2 fb^{-1} collected at the CERN LHC with the ATLAS experiment [22]. The Run 1 search at $\sqrt{s} = 8$ TeV used a dataset corresponding to an integrated luminosity of 20.3 ± 0.56 fb^{-1} for $H \to Z_d Z_d \to 4\ell$ [23] and was published in [24]. The Run 2 data both extended the search and also incorporates several extensions and improvements.

In the search, same-flavor decays of the Z_d bosons to electron and muon pairs are considered, giving the $4e$, $2e2\mu$, and 4μ final states. Final states including τ leptons are not considered. In the absence of a significant signal, a 95% CL upper limit was set on the model-independent fiducial cross section for the process $H \to Z_d Z_d \to 4\ell$. Also, considering the BSM benchmark model where the SM was extended by an additional $U(1)_d$ gauge symmetry, upper limits could be set on the branching ratio BR($H \to Z_d Z_d$) [5, 6]. The search is restricted to the mass range where the Z_d from the decay of the Higgs boson is on-shell, i.e. $15\,\mathrm{GeV} < m_{Z_d} < m_H/2$, where $m_H = 125$ GeV. The Run 2 paper [22] also considered the search $H \to aa \to 4\mu$ where the intermediate state contains two light pseudoscalar bosons, in the range, $1\,\mathrm{GeV} < m_a < 15\mathrm{GeV}$, however this aspect is not part of this proceedings paper.

2. Experimental Setup, Monte Carlo Simulation : Signal and backgrounds

The ATLAS detector covers almost the whole solid angle around the collision point with layers of tracking detectors, calorimeters and muon chambers. Further details can be found in [25]
Signal : The trigger, event pre-selection and lepton reconstruction proceed as desribed in reference [22]. These leptons are then combined into quadruplets according to quality criteria as given below.

Table 1. Summary of the event selection taken from table 1 in [22].

Object	$H \to Z_d Z_d \to 4\ell$
QUADRUPLET SELECTION	- Require at least one quadruplet of leptons consisting of two pairs of same-flavour opposite-charge leptons
	- Three leading-p_T leptons satisfy $p_\mathrm{T} > 20$ GeV, 15 GeV, 10 GeV.
	- At least three muons are required to be reconstructed by combining ID and MS tracks in the 4μ channel.
	- Leptons in the quadruplet responsible for firing at least one trigger
	- $\Delta R(\ell, \ell') > 0.10\ (0.20)$ for all same (different) flavour leptons in the quadruplet
QUADRUPLET RANKING	– Select quadruplet with smallest $\Delta m_{\ell\ell} = |m_{12} - m_{34}|$
EVENT SELECTION	- Reject event if:
	$\quad(m_{J/\Psi} - 0.25\ \mathrm{GeV}) < m_{12,34,14,23} < (m_{\Psi(2S)} + 0.30\ \mathrm{GeV})$
	$\quad(m_{\Upsilon(1S)} - 0.70\ \mathrm{GeV}) < m_{12,34,14,23} < (m_{\Upsilon(3S)} + 0.75\ \mathrm{GeV})$
	- $m_{34}/m_{12} > 0.85$
	- $115\ \mathrm{GeV} < m_{4\ell} < 130\ \mathrm{GeV}$
	- $10\ \mathrm{GeV} < m_{12,34} < 64\ \mathrm{GeV}$
	- $5\ \mathrm{GeV} < m_{14,32} < 75\ \mathrm{GeV}$ for $4e$ and 4μ channels

Simulated event samples are used to model the signal process, and to estimate most of the SM backgrounds. The samples are then passed through a simulation of the ATLAS detector [26] based on GEANT4 [27].

2.1. Signal

$H \to Z_d Z_d \to 4\ell$ The signal process is generated using the Hidden Abelian Higgs Model (HAHM) [9, 10] model in MADGRAPH5 [28] interfaced with PYTHIA8 [29] (v8.170) for the modelling of the parton shower, hadronisation and underlying event (UE), using the CTEQ6L1 parton distribution functions (PDFs) [30] at next-to-leading order (NLO). The mass of the Z_d boson is varied for different signal hypotheses in the range of $15\ \mathrm{GeV} < m_{Z_d} < 60\ \mathrm{GeV}$ for $H \to Z_d Z_d \to 4\ell$, in 5 GeV steps. The considered Higgs boson production mode is gluon-gluon-Fusion (ggF), with a mass $m_H = 125$ GeV. The samples are normalised to the next-to-next-to-next-to-leading-order (N3LO) cross section $\sigma_{SM}(ggF) = 48.58$ pb as recommended by the Higgs cross section working group [31].

2.2. Backgrounds

$H \rightarrow ZZ^* \rightarrow 4\ell$: The POWHEG-BOX v2 MC event generator [32, 33, 34] is used to simulate Higgs production through ggF [35], vector-boson fusion (VBF) [36] and in association with a vector-boson (VH) [37] processes, using the PDF4LHC NLO PDF set [38]. For Higgs boson production in association with a heavy quark pair, events are simulated with MADGRAPH5_AMC@NLO [39], using the CT10nlo PDF set [40] for $t\bar{t}H$ and the NNPDF23 PDF set [41] for $b\bar{b}H$. For the ggF, VBF, VH, and $b\bar{b}H$ production mechanisms,PYTHIA8 [42] is used for the $H \rightarrow ZZ^* \rightarrow 4\ell$ decay as well as for parton showering, hadronisation, and multiple parton-parton interactions using the AZNLO parameter set [43]. For the showering of $t\bar{t}H$ process, HERWIG++ [44] is used with the UEEE5 parameter set [45].

$ZZ^* \rightarrow 4\ell$: The dominant $q\bar{q}$ production mechanism is modelled by POWHEG interfaced toPYTHIA8. The POWHEG-BOX v2 MC event generator [32, 33, 34] is used to simulate Higgs production through ggF [35], vector-boson fusion (VBF) [36] and in association with a vector-boson (VH) [37] processes, using the PDF4LHC NLO PDF set [38]. For Higgs boson production in association with a heavy quark pair, events are simulated with MADGRAPH5_AMC@NLO [39], using the CT10nlo PDF set [40] for $t\bar{t}H$ and the NNPDF23 PDF set [41] for $b\bar{b}H$. For the ggF, VBF, VH, and $b\bar{b}H$ production mechanisms, PYTHIA8 [42] is used for the $H \rightarrow ZZ^* \rightarrow 4\ell$ decay as well as for parton showering, hadronisation, and multiple parton-parton interactions using the AZNLO parameter set [43]. For the showering of $t\bar{t}H$ process, HERWIG++ [44] is used with the UEEE5 parameter set [45].

EWK6 $\rightarrow 4\ell + 2X$: Higher-order electroweak processes (with cross sections proportional to α^6 at leading order) include triboson production and vector-boson scattering, which lead to four leptons in the final state, with two additional particles (quarks, neutrinos, or electrons and muons). These processes are modelled by SHERPA 2.1 with the CT10 PDFs.

$Z + (t\bar{t}/J/\psi/\Upsilon) \rightarrow 4l$: Production of a Z boson, in association with either a quarkonium state ($b\bar{b}$ or $c\bar{c}$) that decays to leptons, or $t\bar{t}$ production with leptonic decays of the prompt W bosons. The processes involving quarkonia are modelled using PYTHIA8 with the CTEQ6L1 PDFs. The $t\bar{t}Z$ process is modelled at leading order with MADGRAPH5 [46] interfaced to PYTHIA8, using the NNPDF 2.3 PDFs [41] and the A14 tune [47].

Reducible background: Processes like $Z + $ jets, $t\bar{t}$ and WZ, produce less than four prompt leptons but can contribute to the selection through objects (e.g. jets) misidentified as leptons. $Z + $ jets events are modeled using SHERPA 2.2. Semi- and fully-leptonic production of $t\bar{t}$ is generated withPOWHEG interfaced to PYTHIA6 [48] for parton shower and hadronisation. The WZ production is modelled by POWHEG interfaced to PYTHIA8 and the CT10 PDFs.

3. Analysis procedure

3.1. Backgrounds to $H \rightarrow XX \rightarrow 4\ell$

The main background contributions come from the $H \rightarrow ZZ^* \rightarrow 4\ell$ and $ZZ^* \rightarrow 4\ell$ processes. These backgrounds are suppressed by the requirements on the lepton invariant masses. They account for 63% and 19% of the total prediction, respectively. Other sources of background with smaller contributions come from higher-order electroweak processes (with cross-sections proportional to α^6 at leading order). These include triboson production and vector-boson scattering, which lead to four leptons in the final state, with two additional particles (quarks, neutrinos, or electrons and muons). They are approximately 17% and 19% of the total prediction for the high- and low- mass selections, respectively. The production of $Z + (J/\psi/\Upsilon) \rightarrow 4\ell$ and $Z + t\bar{t} \rightarrow 4\ell$ constitute another minor source of background, accounting for approximately 1%

of the total. All the background processes described above are estimated from simulation and normalised to the theoretical calculations of their cross sections.

3.2. Sytematics and uncertainties

The identification and quantification of systematics and uncertainties are important in the statistical procedure to identify the significance in the case of discovery and the limit in the case of exclusion.

Luminosity and pile-up: The uncertainty on the integrated luminosity is 3.2%, affecting the overall normalisation.

Lepton-related uncertainties: Uncertainties associated with leptons arise from the reconstruction and identification efficiencies [49, 50], as well as lepton momentum scales and resolutions [51, 50]. The combined effect of all these uncertainties results in an overall normalisation uncertainty in the signal and background of less than 10% (5% in muon final states).

MC background modelling: Uncertainties on the factorisation and renormalisation scales, the parton shower, the choice of PDF and the hadronisation and underlying event model affect those backgrounds normalised with their theory cross sections. Uncertainties on $H \to ZZ^* \to 4\ell$ are found to be between 3% and 9% depending on the Higgs boson production mode, while for Standard Model $q\bar{q}/gg \to ZZ^*$ processes these sources of uncertainties add up to 5%.

Signal modelling: Several sources of systematic uncertainty affect the theoretical modelling of the signal acceptance. Uncertainties originating from the choice of PDFs, the factorisation and renormalisation scales, the modelling of parton shower, hadronisation, and underlying event account for a total effect of 9% [52, 53].

Less than 4 background events are predicted in the signal region for the $H \to Z_d Z_d \to 4\ell$ search, so the dominant uncertainty in the background prediction is the statistical uncertainty.

4. Results

The m_{12} and m_{34} distributions of the selected events are shown in figure 1. The lower triangle represents a loose signal region, and the green shaded area with non-crossed points represents the sigmal region with cuts applied as in Table 1. The crossed points are events that fail the Z veto. This cut is applied onto the alternative-pairing masses m_{32} and m_{14} (relevant only to the 4e and 4μ channels), that they are less than 75 GeV. It is applied to mitigate against any small contributions from SM processes, even in the case of misidentified pairing, where there is Z-boson production with large cross sections. It can be seen that 6 events appear in the signal region where 3.9(3) are expected.
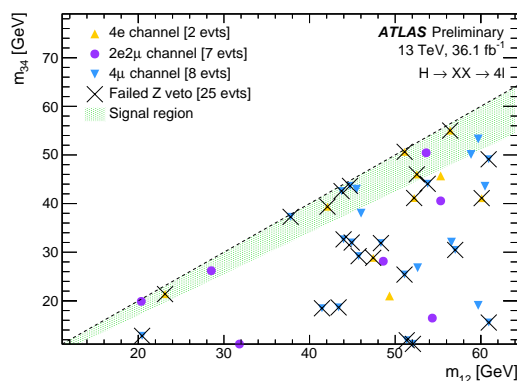

Figure 1. Leading dilepton mass (m_{12}) vs subleading dilepton mass (m_{34}) for events passing the selections (the crossed-through points fail the Z veto) [22].

The biggest deviation from the Standard Model expectation is from a single event at

$\langle m_{\ell\ell}\rangle \approx 20$ GeV, with a local significance of $3.8\,\sigma$. The corresponding global significance is approximately $2.8\,\sigma$, estimated using the likelihood test statistic tail probability approximation described in Ref. [54].

As there is no statistically significant evidence for the signal processes of $H \to Z_d Z_d \to 4\ell$, the results are interpreted in terms of the $Z_d Z_d$ benchmark model [5, 6]. The model provided the signal simulation for computing the reconstruction efficiencies in the fiducial phase spaces defined to mimic the analysis selections described above [22]. Upper limits on the fiducial cross sections should be applicable to any models of 125 GeV Higgs-boson decays to four leptons via two intermediate, on-shell, narrow, promptly-decaying bosons. The fiducial cuts are applied to the four leptons in this decay. These efficiencies are used to compute 95% CL upper limits on the cross sections in the fiducial phase space using the CL_s frequentist formalism [55] with the profile-likelihood test statistic. The results are shown at the left in figure 2.
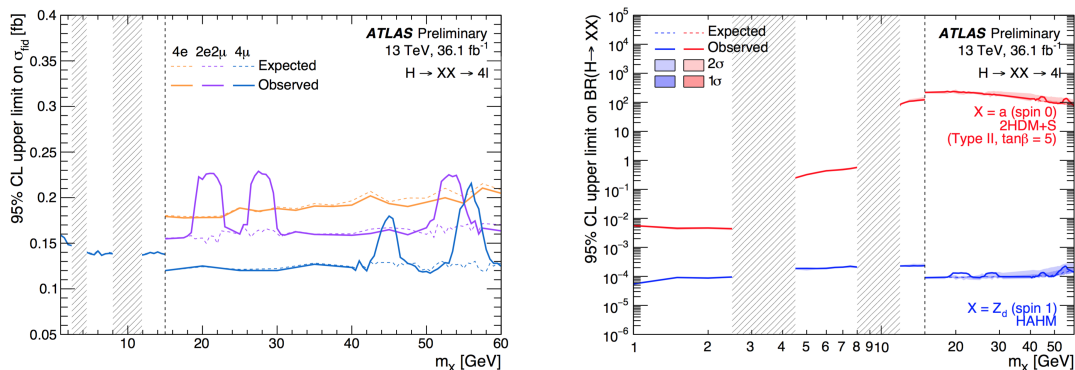

Figure 2. 95% CL upper limits of the process $H \to XX \to 4\ell$ on (left) model-independent fiducial cross sections], and (right) branching fractions BR($H \to Z_d Z_d$) for the benchmark model. The section from 1 to 15 GeV is not discussed in this proceedings article, see [22].

Model-dependent acceptances for the fiducial phase spaces are computed per channel for the $H \to Z_d Z_d \to 4\ell$ search. The acceptances are used in a combined statistical model to compute upper limits on $\sigma_H \cdot \text{BR}(H \to Z_d Z_d \to 4\ell)$. These cross section limits are converted into limits on the branching ratios of $H \to Z_d Z_d$ by using the theoretical branching ratios $Z_d \to \ell\ell$ from the benchmark model [5, 6], and assuming for σ_H the SM cross section[1] for Higgs boson production at $\sqrt{s} = 13$ TeV [53]. The limits on these branching ratios are shown at the right in figure 2 for the $H \to Z_d Z_d \to 4\ell$ search. The branching ratio limit $H \to Z_d Z_d$ is improved over the Run 1 result of Ref. [56] by about a factor of four which corresponds to the increase in both luminosity and Higgs cross section between Run 1 and Run 2.

5. Conclusion

This proceedings article presents a dedicated search for exotic decays of the Standard Model Higgs boson with a mass of 125 GeV to two new spin-one particles, $H \to Z_d Z_d$, which in all cases decay promptly to two lepton pairs. Six events are observed for a background prediction of 3.9(3). The results are expressed in terms of upper limits on the branching ratios BR($H \to Z_d Z_d$) as a function of Z_d mass for the HAHM benchmark model. Limits are also provided on model-independent fiducial cross sections.

6. Acknowledgments

[1] Assumes the presence of BSM decays of the Higgs boson does not alter the SM Higgs-boson production cross section.

References

[1] Fayet P 2004 *Phys.Rev.* **D 70** 023514 (*Preprint* `hep-ph/0403226`)
[2] Finkbeiner D P and Weiner N 2007 *Phys.Rev.* **D 76** 083519 (*Preprint* `astro-ph/0702587`)
[3] Arkani-Hamed, N et al 2009 *Phys.Rev.* **D 79** 015014 (*Preprint* `0810.0713`)
[4] Dudas E *et al.* 2012 *J. High Energy Phys.* **1210** 123 (*Preprint* `1205.1520`)
[5] Curtin D, Essig R, Gori S and Shelton J 2015 *J. High Energy Phys.* **1502** 157 (*Preprint* `1412.0018`)
[6] Curtin D *et al.* 2014 *Phys.Rev.* **D 90** 075004 (*Preprint* `1312.4992`)
[7] Davoudiasl H, Lee H S, Lewis I and Marciano W J 2013 *Phys.Rev.* **D 88** 015022 (*Preprint* `1304.4935`)
[8] Davoudiasl H, Lee H S and Marciano W J 2012 *Phys.Rev.* **D 85** 115019 (*Preprint* `1203.2947`)
[9] Wells J D 2008 (*Preprint* `0803.1243`)
[10] Gopalakrishna S, Jung S and Wells J D 2008 *Phys.Rev.* **D 78** 055002 (*Preprint* `0801.3456`)
[11] Clowe D *et al.* 2006 *Astrophys.J.* **648** L109–L113 (*Preprint* `astro-ph/0608407`)
[12] Adriani O *et al.* 2009 *Nature* **458** 607–609 (*Preprint* `0810.4995`)
[13] Chang J *et al.* 2008 *Nature News* **456** 362
[14] Aguila M *et al.* 2013 *Phys. Rev. Lett.* **110**(14) 141102
[15] Hook A, Izaguirre E and Wacker J G 2011 *Adv.High Energy Phys.* **2011** 859762 (*Preprint* `1006.0973`)
[16] Hoenig I, Samach G and Tucker-Smith D 2014 *Phys.Rev.* **D 90** 075016 (*Preprint* `1408.1075`)
[17] Englert F and Brout R 1964 *Phys. Rev. Lett* **13** 321–323
[18] Higgs P W 1964 *Phys. Rev. Lett* **13** 508–509
[19] Guralnik G S, Hagen C R and Kibble T W B 1964 *Phys. Rev. Lett* **13** 585–587
[20] ATLAS Collaboration 2012 *Phys.Lett.* **B716** 1–29 (*Preprint* `1207.7214`)
[21] CMS Collaboration 2012 *Phys.Lett.* **B716** 30–61 (*Preprint* `1207.7235`)
[22] ATLAS Collaboration 2017 (*Preprint* `http://inspirehep.net/record/1609519`)
[23] ATLAS Collaboration 2013 *Eur.Phys.J.* **C73** 2518 (*Preprint* `1302.4393`)
[24] Wells J D 2015 (*Preprint* `1505.07645`)
[25] ATLAS Collaboration 2009 (*Preprint* `0901.0512`)
[26] ATLAS Collaboration 2010 *Eur. Phys. J. C* **70** 823 (*Preprint* `1005.4568`)
[27] Agostinelli S *et al.* 2003 *Nucl. Instrum. Meth.* **A506** 250–303
[28] Alwall J *et al.* 2011 *J. High Energy Phys.* **1106** 128 (*Preprint* `1106.0522`)
[29] Sjostrand T, Mrenna S and Skands P Z 2008 *Comput.Phys.Commun.* **178** 852–827 (*Preprint* `0710.3820`)
[30] Pumplin J *et al.* 2002 *JHEP* **07** 012 (*Preprint* `hep-ph/0201195`)
[31] LHC Higgs Cross Section Working Group and Heinemeyer, S et al CERN, Geneva, 2013 *CERN-2013-004*
[32] Nason P 2004 *JHEP* **11** 040 (*Preprint* `hep-ph/0409146`)
[33] Frixione S, Nason P and Oleari C 2007 *JHEP* **11** 070 (*Preprint* `0709.2092`)
[34] Alioli S, Nason P, Oleari C and Re E 2010 *JHEP* **06** 043 (*Preprint* `1002.2581`)
[35] Hamilton K, Nason P, Re E and Zanderighi G 2013 *JHEP* **10** 222 (*Preprint* `1309.0017`)
[36] Nason P and Oleari C 2010 *JHEP* **02** 037 (*Preprint* `0911.5299`)
[37] Luisoni G, Nason P, Oleari C and Tramontano F 2013 *JHEP* **10** 083 (*Preprint* `1306.2542`)
[38] Butterworth J *et al.* 2016 *J. Phys.* **G43** 023001 (*Preprint* `1510.03865`)
[39] Alwall J *et al.* 2014 *JHEP* **07** 079 (*Preprint* `1405.0301`)
[40] Lai H L *et al.* 2010 *Phys. Rev.* **D82** 074024 (*Preprint* `1007.2241`)
[41] Ball R *et al.* 2013 *Nucl. Phys. B* **867** 244–289
[42] Sjöstrand T, Mrenna S and Skands P Z 2008 *Comput. Phys. Commun.* **178** 852–867 (*Preprint* `0710.3820`)
[43] ATLAS Collaboration 2014 *JHEP* **09** 145 (*Preprint* `1406.3660`)
[44] Bahr M *et al.* 2008 *Eur. Phys. J.* **C58** 639–707 (*Preprint* `0803.0883`)
[45] Seymour M H and Siodmok A 2013 *JHEP* **10** 113 (*Preprint* `1307.5015`)
[46] Alwall J *et al.* 2011 *JHEP* **06** 128 (*Preprint* `1106.0522`)
[47] ATLAS Collaboration 2014 ATL-PHYS-PUB-2014-021 URL `http://cdsweb.cern.ch/record/1966419`
[48] Sjöstrand T, Mrenna S and Skands P Z 2006 *JHEP* **05** 026 (*Preprint* `hep-ph/0603175`)
[49] ATLAS Collaboration 2017 *Eur. Phys. J. C* **77** 195 (*Preprint* `1612.01456`)
[50] ATLAS Collaboration 2016 *Eur. Phys. J. C* **76** 292 (*Preprint* `1603.05598`)
[51] ATLAS Collaboration 2016 ATL-PHYS-PUB-2016-015 URL `https://cds.cern.ch/record/2203514`
[52] LHC Higgs cross section working group, Dittmaier, S et al 2011 *CERN-2011-002* (*Preprint* `1101.0593`)
[53] LHC Higgs cross section working group, Dittmaier, S et al 2012 *CERN-2012-002* (*Preprint* `1201.3084`)
[54] Gross E and Vitells O 2010 *Eur. Phys. J.* **C70** 525–530 (*Preprint* `1005.1891`)
[55] Read A L 2002 *Journal of Physics G* **28** 2693 URL `http://stacks.iop.org/0954-3899/28/i=10/a=313`
[56] ATLAS Collaboration 2015 *Phys. Rev. D* **92** 092001 (*Preprint* `1505.07645`)